

Adhesive Sulfobetaine Polymer Hydrogels for the Sandwich Cell Culture

Nobuyuki Morimoto,* Atsuki Murata, Yuta Yamamoto, Fumio Narita, and Masaya Yamamoto*

Cite This: *ACS Omega* 2024, 9, 11942–11949

Read Online

ACCESS |



Metrics & More

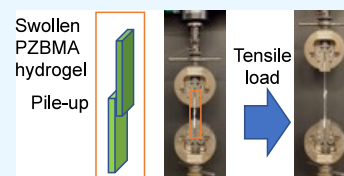


Article Recommendations



Supporting Information

ABSTRACT: Sandwich culture systems are techniques that cultivate cells by sandwiching them between the top and bottom substrates. Since the substrates can be separated, the system is expected to be applied to the construct layering of patterned cells and to the isolation of stacked cells. In this study, we prepared hydrogels composed of zwitterionic sulfobetaine polymers, poly[2-(2-(methacryloyloxyethyl)dimethylammonio)ethyl-1-sulfate] (PZBMA). The ZBMA homopolymers have been shown to form aggregates in aqueous solutions due to their intermolecular interactions. The water content of the PZBMA hydrogels in water was ~70% regardless of *N,N'*-methylenebis(acrylamide), BIS, content as the cross-linker. The results indicated that the intermolecular interaction contributed more to the swelling behaviors than the chemical cross-linker. However, PZBMA hydrogels with 0.1 mol % BIS showed not only high elongation (~850%) properties but also high adhesiveness and self-healing properties. When this PZBMA hydrogel was impregnated with collagen and subjected to sandwich culture using Madin–Darby canine kidney (MDCK) cells, a three-dimensional morphology of MDCK cell aggregates was constructed. Such a sulfobetaine hydrogel is expected to be developed for regenerative medicine.



1. INTRODUCTION

Two-dimensional (2D) monolayer cell culture is a conventional system to evaluate cell functions though the 2D cell culture conditions are insufficient to mimic *in vivo* conditions.¹ As a substitute, three-dimensional (3D) cell culture systems have been developed to construct biological functions similar to those of tissues and organs. Such 3D cell culture systems have been developed in the past decade to form 3D cell aggregates, spheroids, and other structures using noncell-adhesive hydrogels, pendant drops, etc.^{2,3} 3D cell culture systems are proven to be superior to 2D cell culture systems as they resemble the *in vivo* conditions in terms of cell–cell interactions, cell differentiation ability, toxicity, and metabolism of drugs.⁴ However, further developments of these techniques are required for the construction of complex 3D morphologies. Generally, scaffolds are required to place cells in a 3D matrix for the design and fabrication of complex tissues and organs.^{5,6} Such matrices are available; however, the systems are complicated for drug screening or isolation of 3D morphologies for further applications. Simple and utilizing novel techniques are expected using the features of 2D and 3D cell culture systems. Sandwich culture is one of the interesting culture systems that cultivate cells on the top and bottom substrates.^{7–10} The substrates are available as temporal packings and are easy to isolate. Additionally, a variety of 2D substrates with different stiffnesses or alignments can be selected and utilized for precise control. Hydrogels have high water content, similar to our body environment; hence, they can be successfully applied as biomaterials.^{11,12} Generally, hydrogels are fragile with low mechanical properties; therefore, tough hydrogels have been developed since the early

2000s.^{13–15} More recently, various multifunctional hydrogels having superior mechanical properties have been designed. The major additional function is adhesiveness to various substrates. The adhesive behavior can be induced by the substitution of 3,4-dihydroxy-*L*-phenylalanine (DOPA). Due to the ability of DOPA to undergo multiple molecular interactions, DOPA-containing hydrogels can adhere to various material surfaces.¹⁶ Zwitterionic polymers possessing oppositely charged ion pairs in a monomer unit exhibit high water solubility with low protein adsorption and cell adhesion.^{17,18} Among such zwitterionic polymers, our focus is on sulfobetaine polymers because the representative sulfobetaine polymer, poly 3-((2-(methacryloyloxy)ethyl)-dimethylammonio)propane-1-sulfonate, (PSBMA, Figure 1), is known not only for upper critical solution temperature (UCST)-type thermoresponsive behavior but also for its interaction with charged polymers, such as DNA, in addition to its bioinert properties.^{19–21} However, the presence of salts in low concentrations hampers their properties and functions.^{22–24} Therefore, various sulfobetaine polymers with enhanced intra- and interpolymer interactions in the presence of salts have been developed for applications under physiological conditions utilizing their thermoresponsive

Received: December 5, 2023

Revised: January 17, 2024

Accepted: February 20, 2024

Published: March 3, 2024



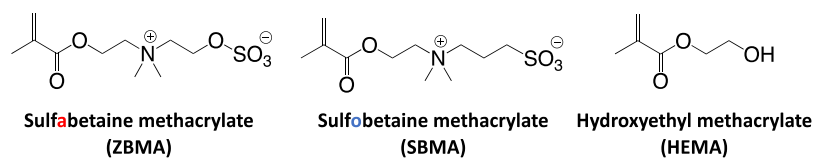


Figure 1. Chemical structures of monomers used in this study.

behavior or aggregated states.^{25–27} Among such polymers, poly[2-(2-(methacryloyloxyethyl)dimethylammonio)ethyl-1-sulfate] sulfobetaine (PZBMA) exhibited thermoresponsive behavior in the presence of salt. In our previous paper, we prepared PZBMA copolymers with PEG methacrylate (molar ratio <5 mol %) to reduce interactions between the polymer chains. The P(ZBMA-*co*-PEG methacrylate) showed multiple thermoresponsiveness under physiological conditions and thermal stabilization of a protein.²⁸ From these results, cross-linking of PZBMA might enhance the interpolymer interaction and obtain a novel type of hydrogel with superior mechanical properties and adhesiveness under physiological conditions. In this study, we prepared PZBMA hydrogels with different cross-linking densities and evaluated the mechanical properties, and finally, the hydrogels were applied to the sandwich cell culture system.

2. MATERIALS AND METHODS

2.1. Materials. 1,3,2-Dioxathiolane 2,2-dioxide, 2-dimethylaminoethyl methacrylate (DMAEMA), and *N,N'*-methylenebis(acrylamide) (BIS) were purchased from Tokyo Chemical Industry (Tokyo, Japan). 2,2-Azobis[2-(2-imidazolin-2-yl)propane]dihydrochloride (VA-044) was purchased from FUJIFILM Wako Pure Chemical Co. (Osaka, Japan). Hoechst 33342 and cell counting kit-8 were purchased from DOJIN Laboratories (Kumamoto, Japan). Collagen type-I solution was purchased from Nitta Gelatin, Inc. (Cellmatrix Type I-A, Osaka, Japan).

2.2. Synthesis of ZBMA Monomer. ZBMA monomer was synthesized according to the previous report.¹⁴ In short, 1,3,2-dioxathiolane 2,2-dioxide (15.0 g, 121 mmol, 1.1 equiv) was dissolved in dry acetonitrile. Then, DMAEMA (17.3 g, 110 mmol, 1.0 equiv) was added dropwise in dry acetonitrile and stirred overnight at room temperature. The precipitate was separated, washed with acetonitrile, and dried in vacuo. Yield: 85.9%

¹H NMR (ECA-600, JEOL Ltd. Tokyo, Japan) in D₂O containing 1 M NaCl: δ (ppm) = 6.12 (s; 1H, *cis* methacrylate CH₂=C(CH₃)CO-), δ = 5.73 (s; 1H, *trans* methacrylate CH₂=C(CH₃)CO-), δ = 4.62 (s; 2H, -COO-CH₂-), δ = 4.48 (s; 2H, -N⁺(CH₃)₂-CH₂CH₂-O-), δ = 3.87–3.85 (m; 2H, -COO-CH₂CH₂-N⁺-), δ = 3.84–3.82 (m; 2H, -N⁺-CH₂-CH₂-O-SO₃⁻), δ = 3.25 (s, 6H, -N⁺(CH₃)₂-CH₂-), δ = 1.89 (s, 3H, δ -methyl CH₂=C(CH₃)CO-).

2.3. Preparation of PZBMA Hydrogels. ZBMA monomer (3.80 g, 13.5 mmol, 100 equiv), cross-linker (BIS: 0.1–1.0 equiv), and the radical initiator (VA-044, 43.7 mg, 0.14 mmol, 1.0 equiv) were dissolved in a mixed solvent of ethanol and acetic acid buffer (0.1 M and pH 4.5) containing 1.0 M NaCl (13.5 mL, 2:8 V/V). Oxygen in the mixture was removed by bubbling nitrogen gas for 15 min. The mixture was poured into a glass mold with a silicone spacer (2 mm thick) and polymerized at 30 °C for 15 h. The residual monomers in the obtained hydrogels were removed against excess water for 7 days.

FT-IR (IRPrestige-21 Shimadzu, Kyoto, Japan) (KBr cm⁻¹): 1719, 1638 ($\nu_{C=O}$), 1472, 1213 (ν_{O-SO_2-O}), 1142 ($\nu_{C=O}$), 1044 ($\nu_{S=O}$).

2.4. Water Content of PZBMA Hydrogels. The obtained hydrogels were punched at sizes of 14 ϕ and equilibrated in Milli-Q water or phosphate-buffered saline (PBS: pH 7.4). Equilibrated hydrogel and the freeze-dried specimens were weighed, and the water content was calculated by using the following equation:

$$\text{water content(\%)} = [W(\text{equilibrated}) - W(\text{freeze-dried}) / W(\text{equilibrated})] \times 100$$

2.5. FE-SEM Observation of PZBMA Hydrogels. Cross sections of PZBMA hydrogels were prepared through freeze fracturing of water-equilibrated hydrogels in liquid nitrogen. The morphology of PZBMA hydrogels with gold-sputtered top surfaces was observed using a field emission scanning electron microscope (FE-SEM, SU-70, Hitachi High-Tech Corporation, Tokyo, Japan).

2.6. Tensile Testing of PZBMA Hydrogels. A tensile test was performed on a Milli-Q-/PBS-equilibrated PZBMA hydrogel specimen using a universal testing machine (Autograph AG-X plus, Shimadzu, Kyoto, Japan) at room temperature. A strip shape specimen (20 × 50 × 2.0 mm) was uniaxially stretched at a strain rate of 100 mm/min. Young's modulus and fracture toughness were evaluated from the stress–strain curve. Four specimens were conducted for each condition.

2.7. Peeling Test of Adhered PZBMA Hydrogels. The adhesion strength of the PZBMA hydrogels was evaluated. Two equilibrated strip-shaped hydrogels (cross-sectional area of 20 × 15 mm) were loaded with a 1.0 kg weight for 1 min in MQ water or PBS. After the weight was removed, the pair of adhered, pile-up hydrogels were tested for a 180° peeling test using the universal tensile testing machine. The fixed the pile-up hydrogels were uniaxially stretched at a strain rate of 100 mm/min.

2.8. Protein Adsorption to PZBMA Hydrogels. Equilibrated swollen PZBMA hydrogels ($\sim\phi$ 10 and 0.2 mm thickness) in PBS were immersed in DMEM containing 10% fetal bovine serum (FBS) for 1 h at room temperature. The hydrogels were rinsed with PBS three times, the adsorbed serum proteins were eluted with 1.0 wt % Triton X-100 solution using an ultrasonic water bath for 30 min, and the quantity of adsorbed protein was determined using the Micro BCA Protein Assay Reagent Kit (Thermo Fisher Scientific, Rockford, IL, USA).

2.9. Cytotoxicity of PZBMA Hydrogels. A silicone tube (OD = 16 mm, ID = 12 mm) was cut into 3 mm lengths and inserted into the bottom of a 24-well plate. Madin–Darby canine kidney (MDCK) cells (5.0 × 10⁵ cells/mL) were preincubated in the well for 24 h. PZBMA hydrogels ($\sim\phi$ 14 and 0.2 mm thickness) were sterilized in ethanol overnight,

Table 1. Characterization of Hydrogels

	mol % of BIS	water content		Young's modulus (kpa)		adhesiveness
		Milli-Q	PBS	Milli-Q	PBS	
PZBMA0.1	0.1	67.1 ± 0.6	62.0 ± 0.7	3.0 ± 0.9	2.5 ± 0.5	+++
PZBMA0.3	0.03	73.6 ± 1.1	68.9 ± 0.8	4.9 ± 1.0	7.7 ± 0.1	+
PZBMA1.0	1.0	70.9 ± 0.3	69.8 ± 0.7	7.8 ± 1.0	7.0 ± 1.4	+
PHEMA1.0	1.0	80.6 ± 0.1	76.8 ± 0.1	2.3 ± 0.3	2.6 ± 0.2	+
PSBMA1.0	1.0	62.9 ± 0.6	86.3 ± 1.0	N.D.	N.D.	-

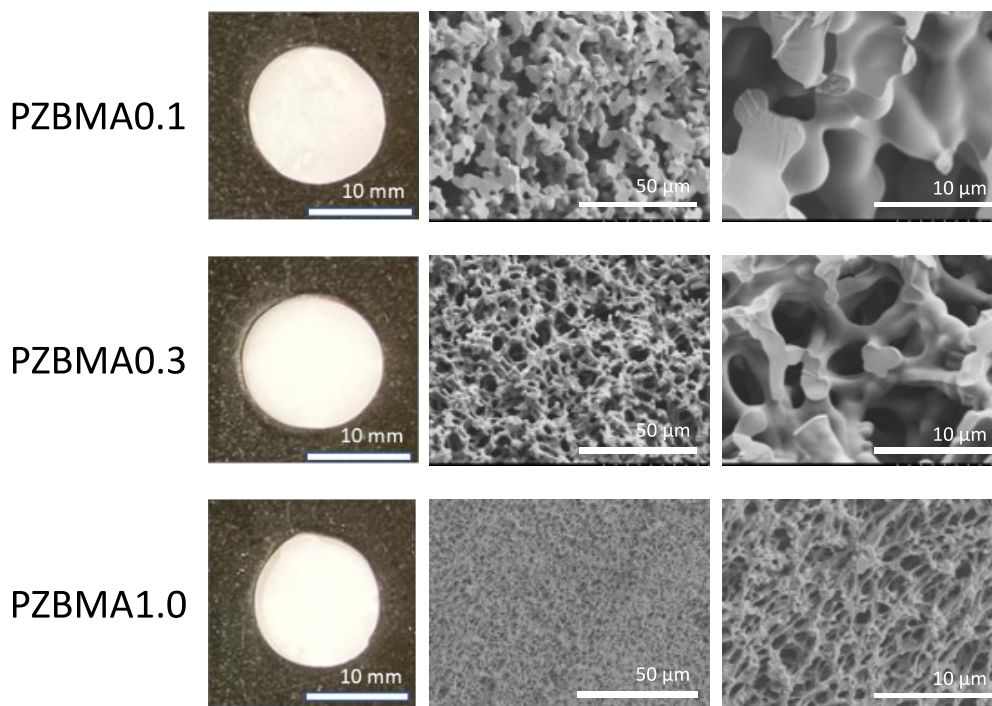


Figure 2. Photo and SEM images of PZBMA hydrogels

and then the solution was replaced by PBS for 5 days. The PZBMA hydrogels were placed over the silicone tube and incubated with the MDCK cells for another 24 h. The cytotoxicity was evaluated by a cell counting kit-8. The procedure was performed based on the manufacturer, and the viability of MDCK cells was estimated by comparison with the absence of hydrogels.

2.10. Preparation of MDCK Cell Aggregates. MDCK cells were dispersed on a 96-well plate at a U-shaped low protein adhesion surface (Prime Surface, Sumitomo Bakelite Co. Ltd., Tokyo, Japan) at a concentration of 3000 cells/well and cultured for 4 days in DMEM containing 10% FBS at 37 °C under 5% CO₂ conditions.

2.11. Preparation of PZBMA Hydrogels for Sandwich Cell Culture. Water-equilibrated PZBMA hydrogels were immersed in ethanol overnight to sterilize the hydrogels. PZBMA hydrogels were equilibrated in PBS, followed by immersion in a collagen type-I solution overnight. The hydrogels were washed with PBS three times, transferred to a 24-well plate, and secured with a glass ring to fix the hydrogels.

2.12. Sandwich Cell Culture. Five wells of MDCK cell aggregates in a 96-well plate were transferred to PZBMA hydrogels and preincubated for 1 day at 37 °C under 5% CO₂ conditions. Then, the MDCK aggregate-plated hydrogels were covered with PZBMA hydrogels equilibrated in DMEM

containing 10% FBS. The effects of collagen coating and sandwich coverage on the growth of MDCK cell aggregates were observed after incubation of 1 and 5 days. Sandwich cultured hydrogels were peeled off, and the MDCK cells on the bottom side of MDCK hydrogels were washed with PBS, fixed in 4% paraformaldehyde for 30 min at 4 °C, and permeabilization was performed with 0.5% Triton X-100 for 10 min. After fixing the cells, they were treated with 1% bovine serum albumin (BSA) as a blocking agent and then stained with Hoechst 33342 (nucleus) and phalloidin-rhodamine for 1 h at room temperature in the dark. The obtained specimens were observed through confocal laser scanning microscopy (CLSM, FV-1000, Olympus, Tokyo, Japan).

3. RESULTS AND DISCUSSION

3.1. Preparation of PZBMA Hydrogels. The PZBMA hydrogels were prepared at molar ratios of 0.1%, 0.3%, and 1.0% of *N,N'*-methylenebis(acrylamide) (BIS) as the cross-linker (Table 1). The 1.0 mol % BIS containing PZBMA hydrogels are represented as PZBMA1.0. For comparison, PSBMA1.0 and poly(2-hydroxyethyl methacrylate) (PHEMA)1.0 were also prepared. The hydrogels of PSBMA0.1 and PSBMA0.3 were quite difficult to handle because of their highly swollen and fragile properties. After removing salt and nonreacted monomers, the obtained PZBMA hydrogels were turbid in Milli-Q water (Figure 2).

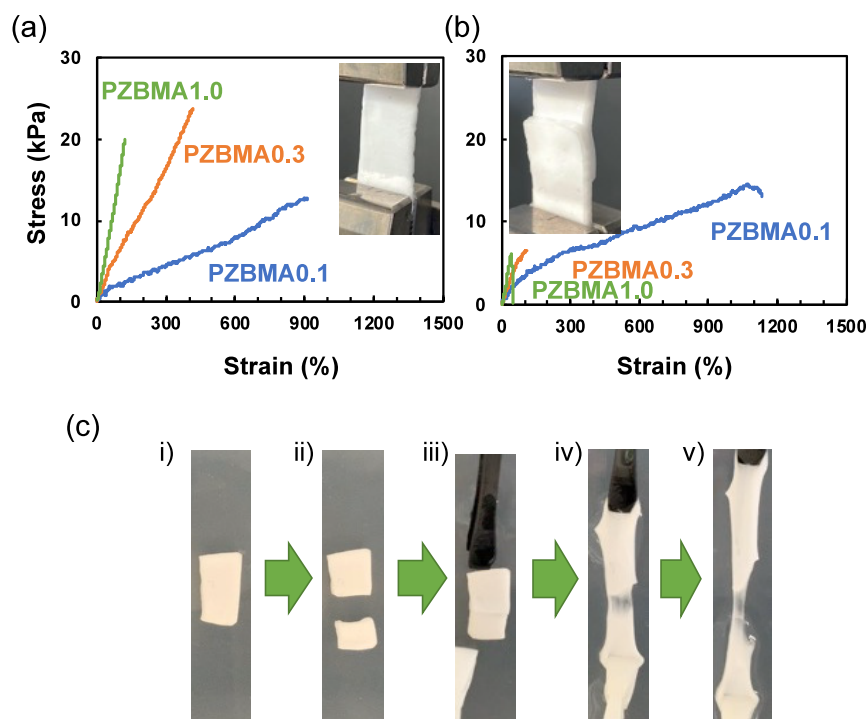


Figure 3. Tensile test profiles of swollen PZBMA hydrogels in PBS. The specimens were (a) single hydrogels with a rectangular shape and (b) adhesive strength between the same hydrogels with 15 mm of the overlapped area. (c) Self-healing behavior of PZBMA0.1. (i) Swollen hydrogel in PBS, (ii) cutting the hydrogel by scissors, (iii) contacting the cutting cross sections using a tweezer and allowing to stand in PBS for 10 min (iv), and (v) pulling with tweezers from both sides.

The water contents of PZBMA hydrogels were evaluated in Milli-Q water and phosphate-buffered saline (PBS). Interestingly, the water content of PZBMA0.1, which has the lowest quantity of the cross-linker, was marginally lower than PZBMA0.3 and PZBMA1.0. The water content was lower in PBS than in Milli-Q water. Though the physiological salt concentration affected the UCST behavior of the semidiluted ZBMA polymer solution, it was insufficient to increase the water content of the PZBMA hydrogels. The plausible explanation is that the ion–dipole interaction has a dynamic equilibration and stabilizes the interactions among polymer chains in the hydrogel network.

In construct, PSBMA1.0 was slightly unclear in Milli-Q water (Figure S2) and increased the transparency and the water content in PBS from 62.9% to 86.3%. PSBMA1.0 indicated that the interaction among polymer chains was reduced by the substitution of dipole–dipole interaction for ion–dipole interaction and increased water content. The result is an effect called the antipolyelectrolyte effect, which enhances the solubility of zwitterionic polymers by the addition of salts.²⁹ Then PZBMA0.1 was immersed in NaCl solution with various concentrations to confirm the effects of salts on the water content in the PZBMA0.1. The relative water contents against Milli-Q water are shown in Figure S3. The water contents were almost comparable or rather lower to that of Milli-Q water below 1.0 M and increased $\sim 135\%$ at 1.5 M of NaCl solution. These results indicated that PZBMA0.1 also exhibited the antipolyelectrolyte effect. Here, the difference in monomer structures between PZBMA and PSBMA hydrogels is only the sulfate group or sulfonate group as the anionic units. These findings indicated that the sulfate group in PZBMA hydrogels might have enhanced electrostatic interaction for both dipole–dipole and monopole–dipole interactions.³⁰

Freeze-dried PZBMA hydrogel specimens were observed by using a scanning electron microscope (SEM). As shown in Figure 2, noticeable structural differences were found in the hydrogels with a degree of BIS concentration. In the case of PZBMA1.0, a fiber-like network structure was observed as usually found in chemically cross-linked hydrogels. On the contrary, a typical structure of randomly linked microspheres and a void among microspheres was observed in the case of PZBMA0.1. The microspheres were solid with $\sim 3 \mu\text{m}$ diameter. These results indicated that the mechanism of the hydrogel formation was different depending on the cross-linking density. The competing chemical cross-linking and other molecular interactions among generated polymer chains during polymerization might be the cause of this difference. The PZMBA0.1 might first form microspheres, which subsequently undergo reaction among themselves. In the case of PZBMA0.3, the structural features of both PZBMA0.1 and PZBMA1.0 were observed. The structure of PZBMA0.3 consisted of a thick network structure with smaller microspheres ($\sim 1 \mu\text{m}$) in the network fibers.

3.2. Mechanical Properties of Swollen PZBMA Hydrogels. Mechanical properties of the hydrogels at equilibrium swelling in water and PBS were evaluated through universal tensile testing. The head speed was set at 100 mm/min to avoid drying of the hydrogels. Figure 3 shows the stress–strain curve of the PZMBA hydrogels swollen in PBS. The curves were mostly linear up to the breaking of the hydrogels. Tensile stress at the break ranged from 10 to 20 kPa. The elastic modulus and elongation at their breaking points corresponded to the concentration of the cross-linker.

At a lower concentration (0.1 mol %) of BIS, the elongation at break was $748.9 \pm 85.7\%$ with a tensile strength of 12.2 ± 0.6 kPa. Compared to PZBMA1.0, the strain of PZBMA0.1

was ~ 6.3 times greater. In the case of PSBMA1.0, the tensile strength could not be evaluated, because of its fragile nature. PHEMA1.0 showed behavior similar to that of PZBMA1.0 during the tensile test.

On the contrary, different tensile behaviors were found in Milli-Q water-swollen hydrogels except for PHEMA1.0. In PZBMA1.0, elastic modulus and stress at break were lower than 30% of their values when swollen in PBS (Table S1). However, the values were higher in the cases of PZBMA0.1 and PZBMA0.3. The tensile stress profiles of the PZBMA hydrogels were different during Milli-Q hydration and PBS hydration. Specifically, in the case of PZBMA0.1, a natural rubber-like deformation profile was found when hydrated by Milli-Q water and exhibited higher values of tensile strength and elongation at break than when hydrated by PBS. The addition of salt indicated the reduction in dipole–dipole interactions among the polymer side chains induced by zwitterionic units. In PZBMA1.0, which has a higher degree of chemical cross-linking, PBS increased elastic modulus and maximum stress. Whereas, the lower degree of chemical cross-linking in PZBMA0.1 and PZBMA0.3 decreased the elongation modulus and stress at the break by swelling in PBS. Norioka et al. reported that poly(acrylamide) hydrogels, prepared with a conventional method at a high monomer concentration and a low cross-linker density, showed a large elongation by inducing the formation of polymer entanglements that resulted in the energy dissipation.³¹ In this study, the preparation concentration was a standard condition ($[ZBMA] = 1.0$ M); however, low cross-linking density and the dipole–dipole interaction between ZBMA polymer chains could enhance the polymer chain entanglements and function the energy dissipation as a mobile cross-linker.

3.3. Adhesive Properties of PZBMA Hydrogels. During the purification of the hydrogels, PZBMA0.1 exhibited an adhesive property when in contact with another PZBMA0.1. Although PZBMA0.1 did not adhere to glassware in an aqueous media. To evaluate the adhesive property, a 1 kg weight was put on the partly pile-up (overlap margin: 15 mm) hydrogels for 1 min in the aqueous media to obtain the specimen, and tensile testing was conducted on the specimen. The results of the PBS-equilibrated PZBMA hydrogels are shown in Figure 3 and Table 2. The elastic moduli of the

profile was similar to linearly increasing stress over a strain range of 250%–900%. The pile-up PZBMA0.1 peeled off from the maximum stress of $\sim 1050\%$ of the strain. This phenomenon also indicated how strong the adhesive force was. Actually, some of the specimens were broken from the nonpile-up area of the hydrogels. On the contrary, pile-up PZBMA0.3 and pile-up PZBMA1.0 were easily peeled off at lower stress and strain than those of the single hydrogel breaking points. The results clearly indicate that the highly mobile polymer chain with the low cross-linking degree played a key role in adhesiveness, as found in the standard tensile test for single hydrogels. PHEMA1.0 also exhibited adhesiveness; the adhesive force might be mainly derived from the hydrogen bond between the hydroxy groups in the side chain; however, the adhesive property was not so strong, at least under the pretreatment condition. Interestingly, the PZBMA hydrogels showed minor adhesiveness in the Milli-Q and PBS solutions toward various substrates, including stainless steel, PP and other plastics, silicone, and skin. The adhesive characteristic of PZBMA0.1 was completely different from DOPA-modified hydrogels.¹⁶ Adhesion behavior toward only the same hydrogels is an important property for encapsulation, avoiding nonspecific adhesion. Such a self-adhesive behavior of PZBMA0.1 is necessary for its self-healing function. Therefore, PZBMA0.1 was cut into two and then contacted face to face with the cross-section. The demonstration is shown in Figure 3c. As found in the case of the adhesion test, self-healing behavior was observed just after the contact. After immersion of PZBMA0.1 in PBS solution for ~ 10 min, the adhesive behavior was stabilized. There are some previous reports regarding PSBMA hydrogels with self-healing properties.^{32–34} These hydrogels are reinforced using comonomers and cross-linkers to enhance their intermolecular interactions. As a result, the PSBMA-based hydrogels adhered to various materials such as glass.

3.4. Sandwich Cell Culture Using PZBMA Hydrogels. Finally, we intended to apply the PZBMA hydrogels as a sandwich cell culture substrate using their self-adhesive property. Generally, sulfobetaine polymers are known for their antifouling properties such as reduced nonspecific protein adsorption and cell adhesion.^{17,18} However, the PZBMA hydrogels have interesting microstructures, as shown in Figure 2. Hence, we performed the adsorption of bovine serum proteins in/on the PZBMA hydrogels. After immersion for 1 h in a 10% serum-containing medium, the adsorbed total proteins in/on the PZBMA hydrogels were evaluated. PZBMA hydrogels exhibited much reduced protein adsorption than the other hydrogels (Figure 4a; $<20\%$ vs PHEMA and $<35\%$ vs PSBMA). These results indicated that the PZBMA hydrogels possessed superior bioinert properties. Followed by evaluation of the protein adsorption, the cytotoxicity of PZBMA hydrogels was evaluated. Here, Madin–Darby canine kidney (MDCK) cells were selected for the sandwich culture. The MDCK cell was derived from a normal dog kidney and is known to exhibit various 3D morphologies of dome and lumen.^{35–38} The morphologies are controlled by physical and chemical stimuli against MDCK cells. MDCK cells were cultured in a monolayer in a 24-well inserted with a silicone tube, and then the PZBMA hydrogel was put on the silicone tube in the culture medium. The cytotoxicity was evaluated after 24 h of cocultivation. As shown in Figure 4b, no significant cell viability was found in the presence of PZBMA hydrogels. Based on these results, we performed the sandwich

Table 2. Mechanical Properties of Pile-Up PZBMA Hydrogels Determined by Tensile Tests

		Young's modulus (kpa)	tensile strength at detach (kpa)	strain at detach (%)
PZBMA0.1	MQ	3.0 \pm 0.9	16.3 \pm 8.8	609 \pm 175
	PBS	2.5 \pm 0.5	13.1 \pm 2.8	988 \pm 23
PZBMA0.3	MQ	4.9 \pm 1.0	5.6 \pm 1.0	171 \pm 20
	PBS	7.7 \pm 0.1	6.7 \pm 1.2	114 \pm 5
PZBMA1.0	MQ	7.8 \pm 1.0	4.2 \pm 0.5	63 \pm 20
	PBS	7.0 \pm 1.4	8.0 \pm 2.0	61 \pm 19

hydrogels were comparable to those of the results of the tensile test for the corresponding single hydrogels. Interestingly, only PZBMA0.1 exhibited preferable adhesive properties. Initially, up to 200% of the strain, the loading stress of pile-up PZBMA0.1 was approximately 2-fold higher than that of single PZBMA0.1 without adhesion. The profile of pile-up PZBMA0.1 indicated that the thickness at the overlap area was doubled due to the effect of adhesiveness. The loading

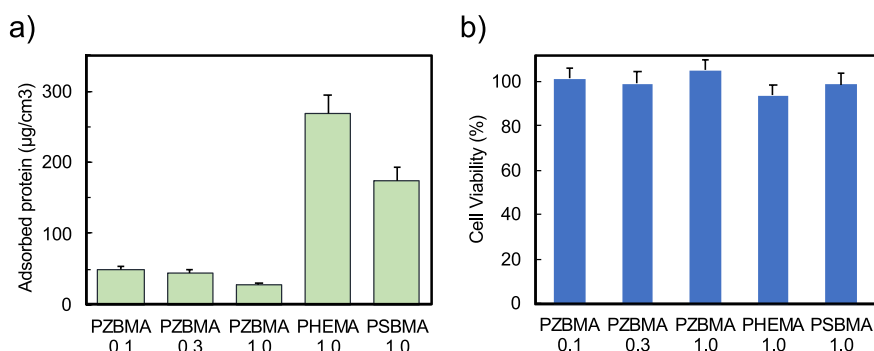


Figure 4. (a) Total amount of adsorbed protein to hydrogels after 60 min contact with 10% FBS. (b) MDCK cell viability in the presence of hydrogels after 24 h incubation at 37 °C, 5% CO₂.

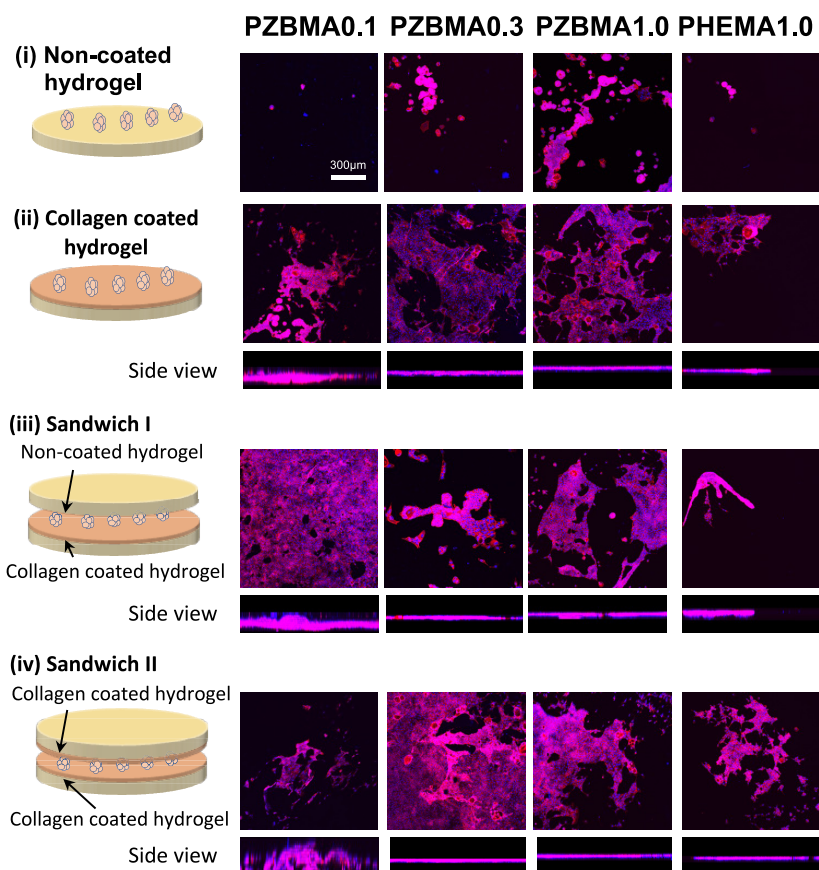


Figure 5. Sandwich cell culture of MDCK cells on PZBMA hydrogels after incubation of the spheroids for 5 days. (i) Nontreated, (ii) collagen coated, (iii) sandwich of collagen coated (bottom) and nontreated (top), and (iv) sandwich of collagen coated (bottom and top) PZBMA hydrogels.

cell culture using PZBMA hydrogels. Even with the low cytotoxicity of PZBMA hydrogels, the lower cell adhesive property was of concern. Therefore, collagen type-I was impregnated onto PZBMA hydrogels before performing the sandwich cell culture to avoid the detachment of the cells. The MDCK cell culture was initially prepared through 3D cell aggregation in a low-protein-adsorbed 96-well plate and transferred to the hydrogels after 4 days of incubation. Four series of hydrogel–cell interfaces were prepared to elucidate the effects of sandwich culture: (i) nontreated hydrogel, (ii) collagen-coated hydrogel, (iii) sandwich culture of nontreated hydrogel (top) and collagen-coated hydrogel (bottom), and (iv) sandwich culture between collagen-coated hydrogels (top and bottom). When the hydrogels were sandwiched between

the cell aggregates, only the edges of the hydrogels were pressed using a cylindrical-shaped jig to avoid crushing the cells to death. After 1 day of incubation on the hydrogels, only some spheroids and dissociated cells were found on the nontreated samples. The spheroids could not adhere or adhere to weak interactions and were washed out from the surface. Through collagen type-I coating, as shown in series II–IV, the number of adherent cells in the case of PZBMA hydrogels increased (Figure S4). A small number of aggregated cells was adhered on the PZBMA0.1 surface. On the contrary, different cell morphologies on PZBMA0.3 and PZBMA1.0 were observed. The adhered cells on these surfaces were elongated and formed a large aggregation due to MDCK cells. The cell adhesion in the case of PZBMA hydrogels was better as

compared with the PSBMA and PHEMA hydrogels (Figure S5). The difference might be due to the maintained collagen coating on the hydrogels. Collagen, a basic protein, could strongly interact with PZBMA hydrogels, showcasing its ability to interact under physiological conditions. CLSM images after 5 days of sandwich incubation are shown in Figure 5, where the apparent elongation and proliferation of adherent cells were observed through collagen impregnated on PZBMA hydrogels. In particular, millimeter-sized and three-dimensional (~120 μm in height) structures were observed in the sandwich type-II culture with PZBMA0.1. In the case of sandwich, type-I, the cells were spread over 2D with several dome structures. The results suggested that in the case of PZBMA0.1, the collagen-coated layers on both sides of the sandwich culture made contact and adhered to each other, and both sides were well-adhered as cell substrates, leading to the formation of structures in the 3D direction. As there was less protein adsorption in PZBMA0.3 and PZBMA1.0, it was considered that the hydrogels could only expand in two dimensions, as in the case of collagen coating, due to weak self-adhesion between the hydrogels during sandwich culture. In addition, it has been reported that the softness and fluidity of the hydrogel surface affected the formation of 3D structures, suggesting that the collagen coating on PZBMA0.1 exhibited excellent functionality as a 3D substrate.

4. CONCLUSIONS

In this study, we prepared PZBMA hydrogels from a zwitterionic monomer with a sulfate group in the anionic unit. PZBMA0.1, the lowest composition of chemical cross-linker, the swollen hydrogel exhibited high elongation properties. In addition, PZBMA0.1 showed self-adhesiveness and healing properties in aqueous solution. Using self-adhesive properties, the hydrogels were applied to a sandwich cell culture system with MDCK cells. By impregnation of collagen type-I to PZBMA0.1, thickening of the cell layer and formation of 3D structures were observed. In conclusion, using the self-adhesive hydrogel as a substrate for a simple sandwich culture method is expected to develop as a general semi-3D culture technique for organoid formation.

■ ASSOCIATED CONTENT

SI Supporting Information

The Supporting Information is available free of charge at <https://pubs.acs.org/doi/10.1021/acsomega.3c09708>.

FT-IR spectra of PZBMA hydrogels, optical and SEM images of PSBMA and PHEMA hydrogels, mechanical properties of PZBMA hydrogels, and fluorescence images of MDCK cells after sandwich cell culture on hydrogels (PDF)

Tensile test of swollen and pile-up PZBMA0.1 (MP4)

■ AUTHOR INFORMATION

Corresponding Authors

Nobuyuki Morimoto – Department of Materials Processing, Graduate School of Engineering, Tohoku University, Sendai, Miyagi 980-8579, Japan; Department of Materials for Energy, Shimane University, Matsue, Shimane 690-8504, Japan; orcid.org/0000-0002-7620-3352; Email: morimoto@mat.shimane-u.ac.jp

Masaya Yamamoto – Department of Materials Processing, Graduate School of Engineering, Tohoku University, Sendai,

Miyagi 980-8579, Japan; Graduate School of Biomedical Engineering, Tohoku University, Sendai 980-8579, Japan; orcid.org/0000-0003-0271-291X; Email: masaya.yamamoto.b6@tohoku.ac.jp

Authors

Atsuki Murata – Department of Materials Processing, Graduate School of Engineering, Tohoku University, Sendai, Miyagi 980-8579, Japan

Yuta Yamamoto – Department of Materials Processing, Graduate School of Engineering, Tohoku University, Sendai, Miyagi 980-8579, Japan

Fumio Narita – Department of Frontier Sciences for Advanced Environment, Graduate School of Environmental Studies, Tohoku University, Sendai 980-8579, Japan

Complete contact information is available at:

<https://pubs.acs.org/10.1021/acsomega.3c09708>

Notes

The authors declare no competing financial interest.

■ ACKNOWLEDGMENTS

This work was supported by JKA through its promotion funds from KEIRIN RACE to N.M. and Japan Society for the Promotion of Sciences (JSPS) KAKENHI (#JP22H03969 and #JP22H05394 to N.M.; #JP21H03814 and #JP21H05769 to M.Y.).

■ REFERENCES

- (1) Caliani, S. R.; Burdick, J. A. A Practical Guide to Hydrogels for Cell Culture. *Nat. Methods* **2016**, *13* (5), 405–414.
- (2) Shen, H.; Cai, S.; Wu, C.; Yang, W.; Yu, H.; Liu, L. Recent Advances in Three-Dimensional Multicellular Spheroid Culture and Future Development. *Micromachines (Basel)* **2021**, *12* (1), 96.
- (3) Gencoglu, M. F.; Barney, L. E.; Hall, C. L.; Brooks, E. A.; Schwartz, A. D.; Corbett, D. C.; Stevens, K. R.; Peyton, S. R. Comparative Study of Multicellular Tumor Spheroid Formation Methods and Implications for Drug Screening. *ACS Biomater. Sci. Eng.* **2018**, *4* (2), 410–420.
- (4) Rodrigues, J.; Heinrich, M. A.; Teixeira, L. M.; Prakash, J. 3D In Vitro Model (R)evolution: Unveiling Tumor-Stroma Interactions. *Trends Cancer Res.* **2021**, *7* (3), 249–264.
- (5) Liu, C.; Xia, Z.; Czernuszka, J. T. Design and Development of Three-Dimensional Scaffolds for Tissue Engineering. *Chem. Eng. Res. Des.* **2007**, *85* (7), 1051–1064.
- (6) Ravi, M.; Paramesh, V.; Kaviya, S. R.; Anuradha, E.; Solomon, F. D. P. 3D Cell Culture Systems: Advantages and Applications. *J. Cell. Physiol.* **2015**, *230* (1), 16–26.
- (7) Nattasit, P.; Niibe, K.; Yamada, M.; Ohori-Morita, Y.; Limraksasin, P.; Tiskratok, W.; Yamamoto, M.; Egusa, H. Stiffness-Tunable Hydrogel-Sandwich Culture Modulates the YAP-Mediated Mechanoreponse in Induced-Pluripotent Stem Cell Embryoid Bodies and Augments Cardiomyocyte Differentiation. *Macromol. Biosci.* **2023**, *23*, No. e2300021.
- (8) Foster, E.; You, J.; Siltanen, C.; Patel, D.; Haque, A.; Anderson, L.; Revzin, A. Heparin Hydrogel Sandwich Cultures of Primary Hepatocytes. *Eur. Polym. J.* **2015**, *72*, 726–735.
- (9) Tuschl, G.; Hrach, J.; Walter, Y.; Hewitt, P. G.; Mueller, S. O. Serum-Free Collagen Sandwich Cultures of Adult Rat Hepatocytes Maintain Liver-like Properties Long Term: A Valuable Model for In Vitro Toxicity and Drug-Drug Interaction Studies. *Chem. Biol. Interact.* **2009**, *181* (1), 124–137.
- (10) Bjørge, I. M.; Salmeron-Sanchez, M.; Correia, C. R.; Mano, J. F. Cell Behavior within Nanogrooved Sandwich Culture Systems. *Small* **2020**, *16* (31), No. e2001975.

- (11) Caló, E.; Khutoryanskiy, V. V. Biomedical Applications of Hydrogels: A Review of Patents and Commercial Products. *Eur. Polym. J.* **2015**, *65*, 252–267.
- (12) Cao, H.; Duan, L.; Zhang, Y.; Cao, J.; Zhang, K. Current Hydrogel Advances in Physicochemical and Biological Response-Driven Biomedical Application Diversity. *Signal Transduction Targeted Ther.* **2021**, *6* (1), 426.
- (13) Zhang, Y. S.; Khademhosseini, A. Advances in Engineering Hydrogels. *Science* **2017**, *356* (6337), No. eaaf3627, DOI: 10.1126/science.aaf3627.
- (14) Peak, C. W.; Wilker, J. J.; Schmidt, G. A Review on Tough and Sticky Hydrogels. *Colloid Polym. Sci.* **2013**, *291*, 2031.
- (15) Zhao, X. Multi-Scale Multi-Mechanism Design of Tough Hydrogels: Building Dissipation into Stretchy Networks. *Soft Matter* **2014**, *10* (5), 672–687.
- (16) Zhang, W.; Wang, R.; Sun, Z.; Zhu, X.; Zhao, Q.; Zhang, T.; Cholewinski, A.; Yang, F. K.; Zhao, B.; Pinnaratip, R.; Forooshani, P. K.; Lee, B. P. Catechol-Functionalized Hydrogels: Biomimetic Design, Adhesion Mechanism, and Biomedical Applications. *Chem. Soc. Rev.* **2020**, *49* (2), 433–464.
- (17) Blackman, L. D.; Gunatillake, P. A.; Cass, P.; Locock, K. E. S. An Introduction to Zwitterionic Polymer Behavior and Applications in Solution and at Surfaces. *Chem. Soc. Rev.* **2019**, *48* (3), 757–770.
- (18) Lowe, A. B.; McCormick, C. L. Synthesis and Solution Properties of Zwitterionic Polymers. *Chem. Rev.* **2002**, *102* (11), 4177–4189.
- (19) Morimoto, N.; Muramatsu, K.; Nomura, S.-I. M.; Suzuki, M. Trading Polymeric Microspheres: Exchanging DNA Molecules via Microsphere Interaction. *Colloids Surf. B Biointerfaces* **2015**, *128*, 94–99.
- (20) Ohsugi, A.; Furukawa, H.; Kakugo, A.; Osada, Y.; Gong, J. P. Catch and Release of DNA in Coacervate-Dispersed Gels. *Macromol. Rapid Commun.* **2006**, *27* (15), 1242–1246.
- (21) Kuang, W.; Zhao, X. Synthesis, Characterization, and Properties of Novel Hydrophobically Associating Fluorinated Copolymers for DNA Delivery. *React. Funct. Polym.* **2013**, *73* (5), 703–709.
- (22) Hildebrand, V.; Laschewsky, A.; Päch, M.; Müller-Buschbaum, P.; Papadakis, C. M. Effect of the Zwitterion Structure on the Thermo-Responsive Behaviour of Poly(sulfobetaine Methacrylates). *Polym. Chem.* **2017**, *8* (1), 310–322.
- (23) Morimoto, N.; Muramatsu, K.; Wazawa, T.; Inoue, Y.; Suzuki, M. Self-Assembled Microspheres Driven by Dipole-Dipole Interactions: UCST-Type Transition in Water. *Macromol. Rapid Commun.* **2014**, *35* (1), 103–108.
- (24) Willcock, H.; Lu, A.; Hansell, C. F.; Chapman, E.; Collins, I. R.; O'Reilly, R. K. One-Pot Synthesis of Responsive Sulfobetaine Nanoparticles by RAFT Polymerisation: The Effect of Branching on the UCST Cloud Point. *Polym. Chem.* **2014**, *5* (3), 1023–1030.
- (25) Hildebrand, V.; Laschewsky, A.; Päch, M.; Müller-Buschbaum, P.; Papadakis, C. M. Effect of the zwitterion structure on the thermo-responsive behaviour of poly (sulfobetaine methacrylates). *Polym. Chem.* **2017**, *8* (1), 310–322.
- (26) Vasantha, V. A.; Jana, S.; Parthiban, A.; Vancso, J. G. Water Swelling, Brine Soluble Imidazole Based Zwitterionic Polymers—Synthesis and Study of Reversible UCST Behaviour and Gel-Sol Transitions. *Chem. Commun.* **2014**, *50* (1), 46–48.
- (27) Morimoto, N.; Oishi, Y.; Yamamoto, M. The Design of Sulfobetaine Polymers with Thermoresponsiveness under Physiological Salt Conditions. *Macromol. Chem. Phys.* **2020**, *221* (5), 1900429.
- (28) Morimoto, N.; Yamamoto, M. Design of an LCST-UCST-Like Thermoresponsive Zwitterionic Copolymer. *Langmuir* **2021**, *37* (11), 3261–3269.
- (29) Li, M.; Zhuang, B.; Yu, J. Functional Zwitterionic Polymers on Surface: Structures and Applications. *Chem.—Asian J.* **2020**, *15* (14), 2060–2075.
- (30) Nizardo, N. M.; Schanzenbach, D.; Schönemann, E.; Laschewsky, A. Exploring Poly(ethylene Glycol)-Polyzwitterion Diblock Copolymers as Biocompatible Smart Macrosurfactants Featuring UCST-Phase Behavior in Normal Saline Solution. *Polymers* **2018**, *10* (3), 325.
- (31) Norioka, C.; Inamoto, Y.; Hajime, C.; Kawamura, A.; Miyata, T. A Universal Method to Easily Design Tough and Stretchable Hydrogels. *NPG Asia Mater.* **2021**, *13* (1), 1–10.
- (32) Wang, L.; Gao, G.; Zhou, Y.; Xu, T.; Chen, J.; Wang, R.; Zhang, R.; Fu, J. Tough, Adhesive, Self-Healable, and Transparent Ionically Conductive Zwitterionic Nanocomposite Hydrogels as Skin Strain Sensors. *ACS Appl. Mater. Interfaces* **2019**, *11* (3), 3506–3515.
- (33) Sun, Y.; Lu, S.; Li, Q.; Ren, Y.; Ding, Y.; Wu, H.; He, X.; Shang, Y. High Strength Zwitterionic Nano-Micelle Hydrogels with Superior Self-Healing, Adhesive and Ion Conductive Properties. *Eur. Polym. J.* **2020**, *133*, No. 109761.
- (34) Feng, E.; Gao, W.; Li, J.; Wei, J.; Yang, Q.; Li, Z.; Ma, X.; Zhang, T.; Yang, Z. Stretchable, Healable, Adhesive, and Redox-Active Multifunctional Supramolecular Hydrogel-Based Flexible Supercapacitor. *ACS Sustainable Chem. Eng.* **2020**, *8* (8), 3311–3320.
- (35) Imai, M.; Furusawa, K.; Mizutani, T.; Kawabata, K.; Haga, H. Three-Dimensional Morphogenesis of MDCK Cells Induced by Cellular Contractile Forces on a Viscous Substrate. *Sci. Rep.* **2015**, *5*, 14208.
- (36) Hirashima, T.; Hoshuyama, M.; Adachi, T. In Vitro Tubulogenesis of Madin-Darby Canine Kidney (MDCK) Spheroids Occurs Depending on Constituent Cell Number and Scaffold Gel Concentration. *J. Theor. Biol.* **2017**, *435*, 110–115.
- (37) Cattaneo, I.; Condorelli, L.; Terrinoni, A. R.; Antiga, L.; Sangalli, F.; Remuzzi, A. Shear Stress Reverses Dome Formation in Confluent Renal Tubular Cells. *Cell. Physiol. Biochem.* **2011**, *28* (4), 673–682.
- (38) Shen, Y.; Hou, Y.; Yao, S.; Huang, P.; Yobas, L. In Vitro Epithelial Organoid Generation Induced by Substrate Nanotopography. *Sci. Rep.* **2015**, *5*, 9293.